Soft Matter

SUPPORTING INFORMATION

# Simulation of weak polyelectrolyte brushes: the effects of ionizable monomer fraction and monovalent salt†

Xin Yuan,[a] Shahryar Ramezani Bajgiran,[b] Rahatun Akter,[a] Amanda B. Marciel*[b] and Jeremy C. Palmer*[a]

[a] *Department of Chemical and Biomolecular Engineering, University of Houston, Houston, TX 77204*
[b] *Department of Chemical and Biomolecular Engineering, Rice University, Houston, Texas 77005*
* *E-mails: am152@rice.edu, jcpalmer@uh.edu*

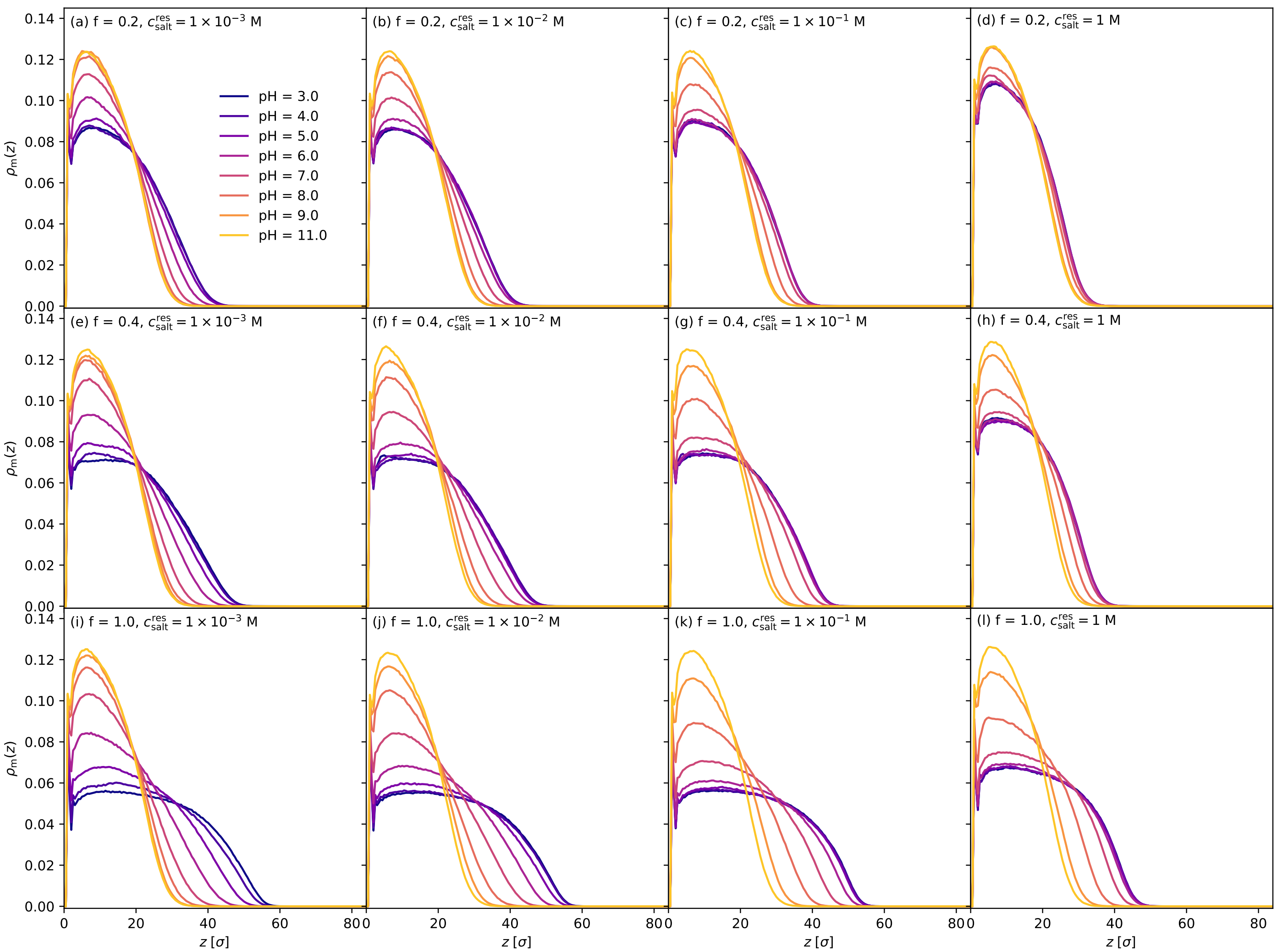


**Fig. S1** Monomer number density $\rho_{\mathrm{m}}(z)$ as a function of the distance from the grafting surface $z$ for polyelectrolyte brushes with ionizable monomer fractions $f$. The pH of the reservoir is reported in the legend in panel (a); the legend applies to all panels. The salt concentration of the reservoir $c_{\mathrm{salt}}^{\mathrm{res}}$ is reported in the label of each panel.

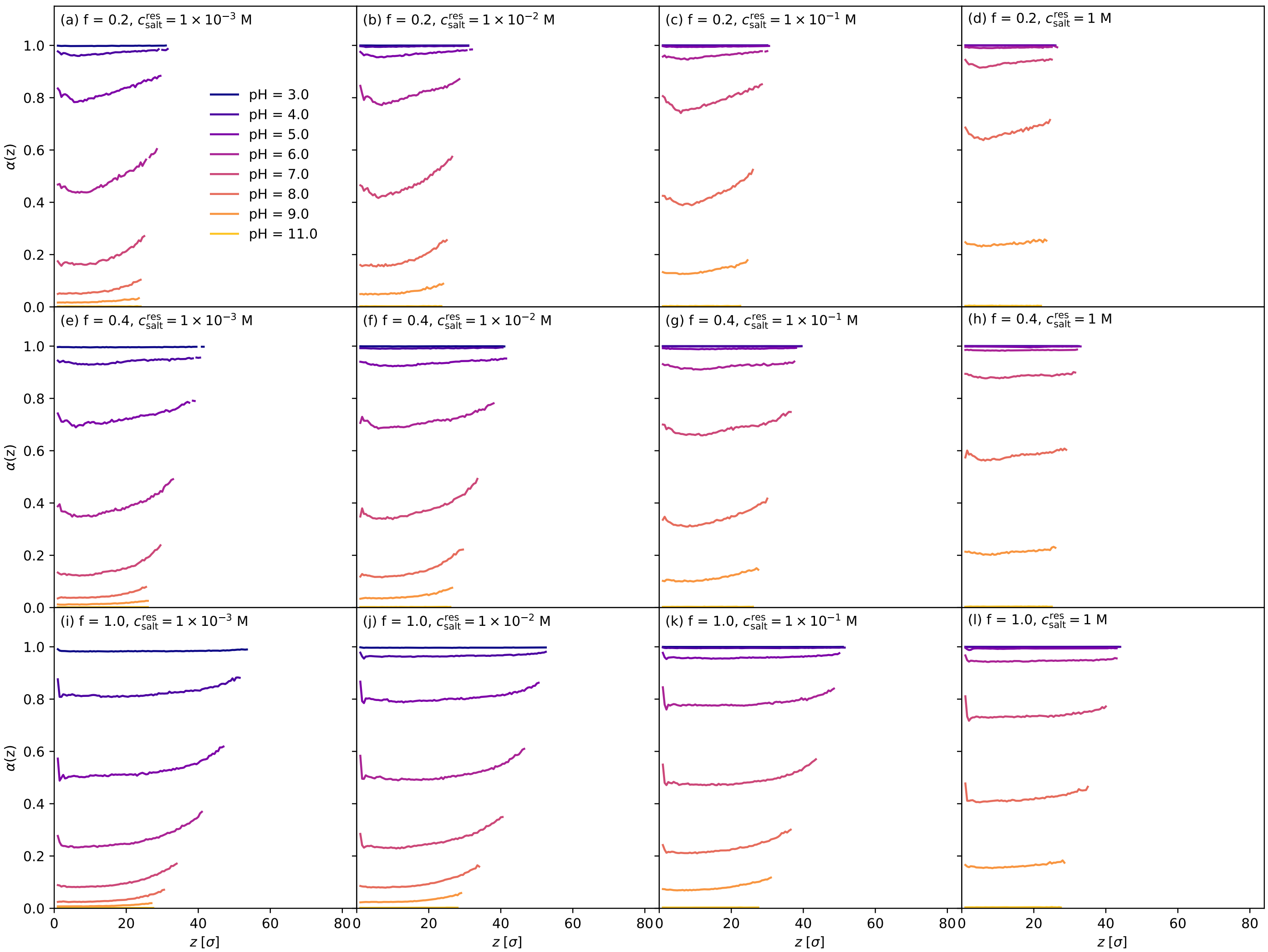


**Fig. S2** Fraction of charged monomers $\alpha(z)$ as a function of the distance from the grafting surface $z$ for polyelectrolyte brushes with ionizable monomer fractions $f$. The pH of the reservoir is reported in the legend in panel (a); the legend applies to all panels. The salt concentration of the reservoir $c_{\mathrm{salt}}^{\mathrm{res}}$ is reported in the label of each panel.

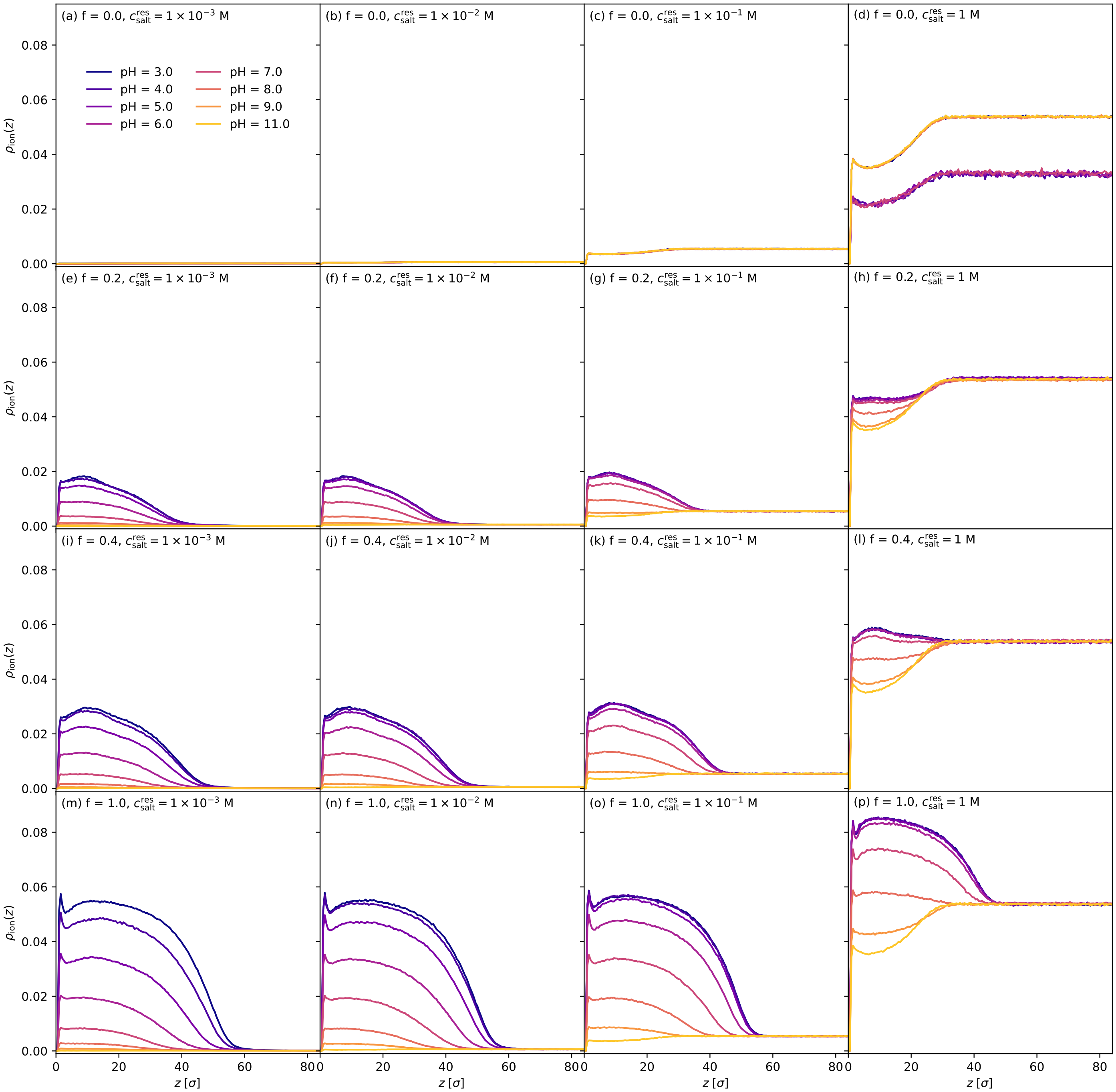


**Fig. S3** The free ion number density $\rho_{\rm ion}(z)$ as a function of the distance from the grafting surface $z$ for polyelectrolyte brushes with ionizable monomer fractions $f$. Free ion species include $Na^+$, $Cl^-$, $H^+$, and $OH^-$. The pH of the reservoir is reported in the legend in panel (a); the legend applies to all panels. The salt concentration of the reservoir $c_{\rm salt}^{\rm res}$ is reported in the label of each panel.

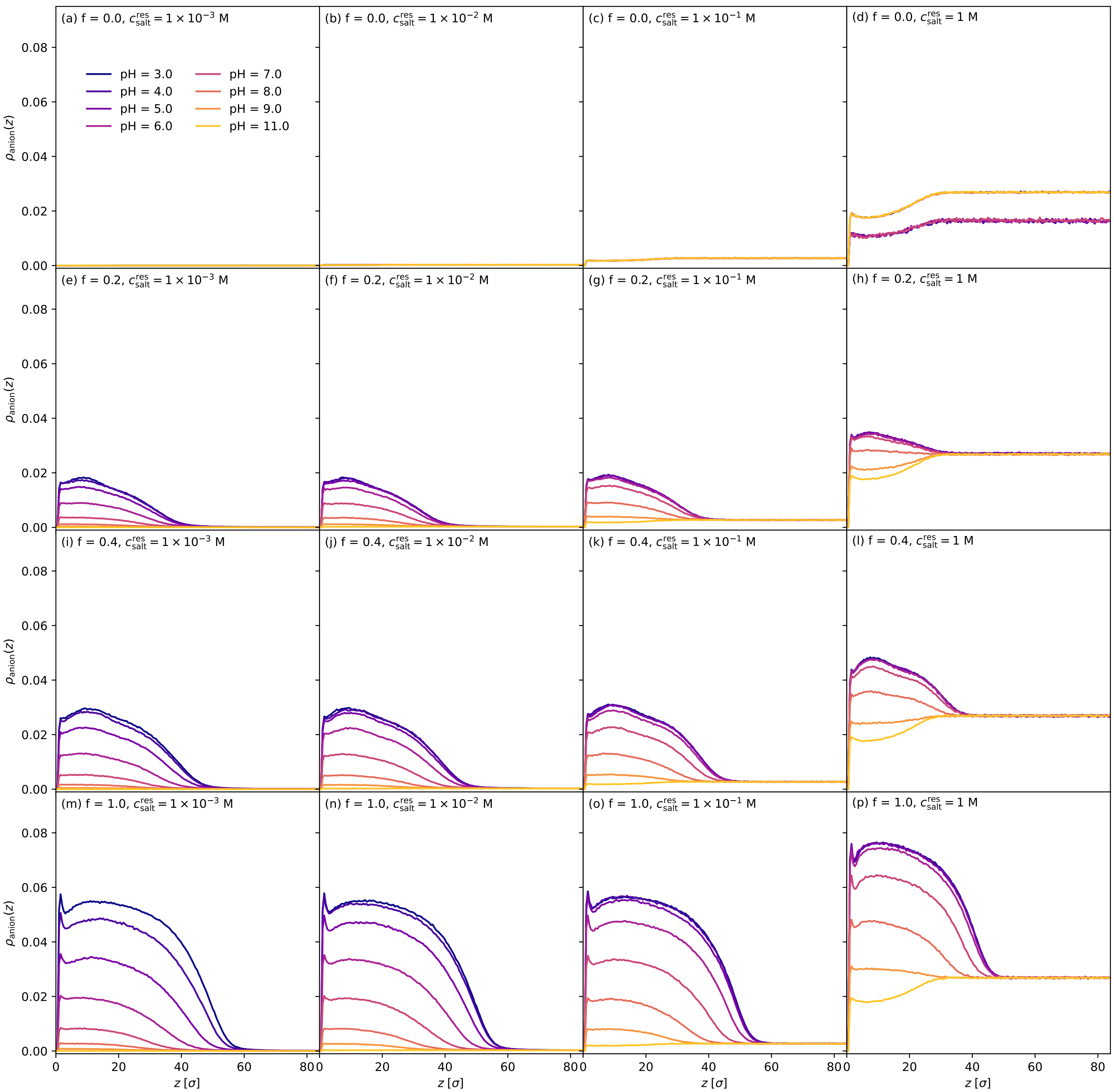


**Fig. S4** The free anion number density $\rho_{\mathrm{anion}}(z)$ as a function of the distance from the grafting surface $z$ for polyelectrolyte brushes with ionizable monomer fractions $f$. Free anion species include $Cl^{-}$ and $OH^{-}$. The pH of the reservoir is reported in the legend in panel (a); the legend applies to all panels. The salt concentration of the reservoir $c_{\mathrm{salt}}^{\mathrm{res}}$ is reported in the label of each panel.

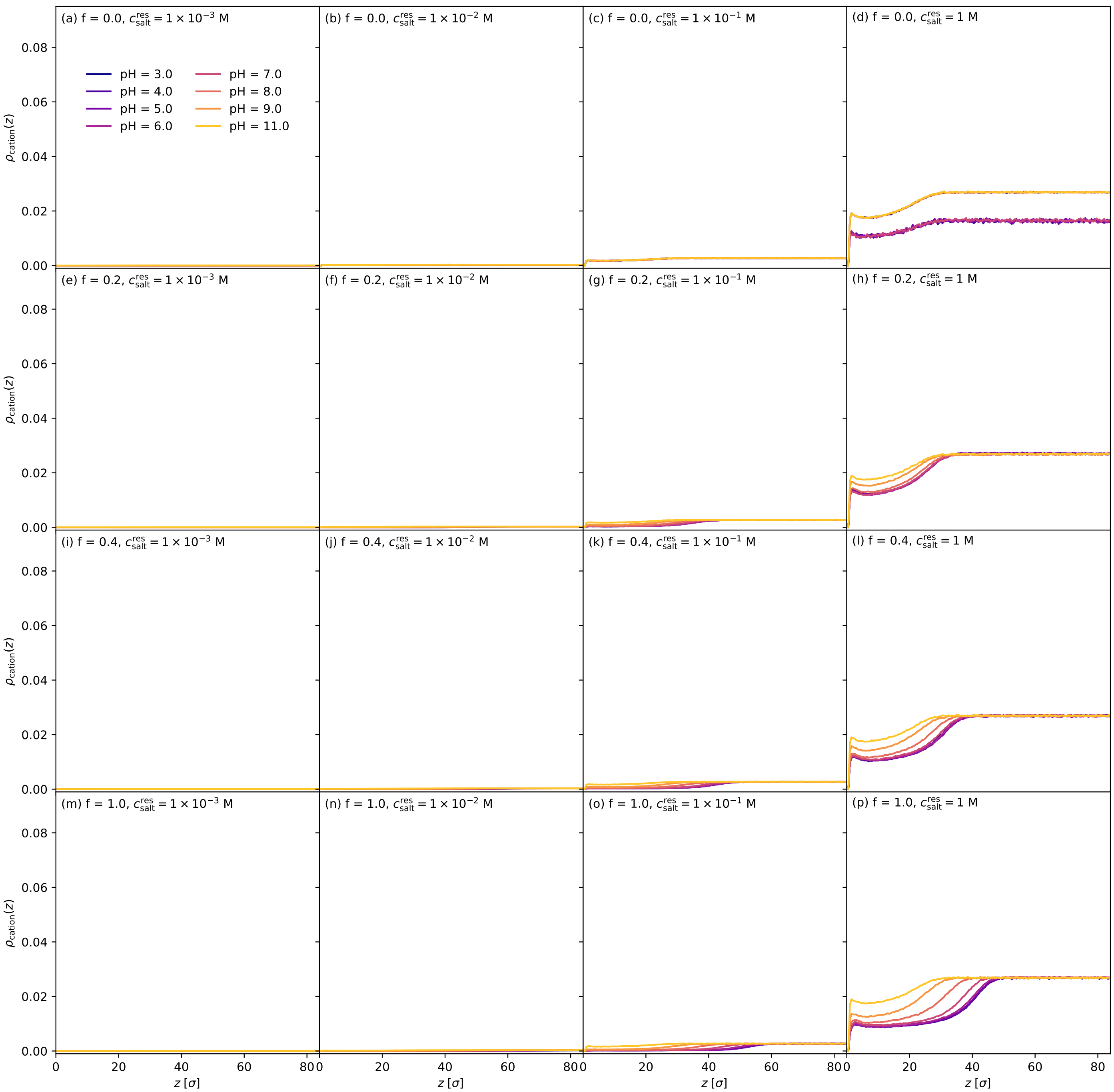


**Fig. S5** The free cation number density $\rho_{\mathrm{cation}}(z)$ as a function of the distance from the grafting surface $z$ for polyelectrolyte brushes with ionizable monomer fractions $f$. Free cation species include $Na^{+}$ and $H^{+}$. The pH of the reservoir is reported in the legend in panel (a); the legend applies to all panels. The salt concentration of the reservoir $c_{\mathrm{salt}}^{\mathrm{res}}$ is reported in the label of each panel.

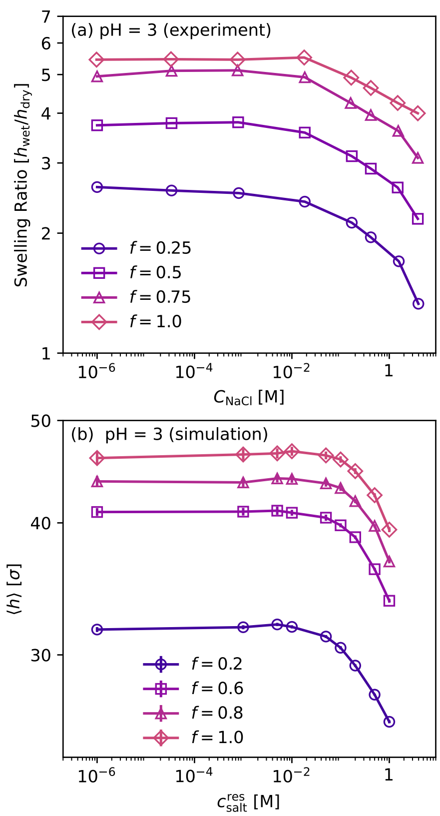


**Fig. S6** (a) Experimental data [from F. Safi Samghabadi, S. Ramezani Bajgiran, M. Villegas Orellana, J. C. Conrad and A. B. Marciel, ACS Macro Letters, 2024, 13, 1570–1576] showing the brush swelling ratio as a function of added salt concentration $c_{\text{salt}}$ for polyelectrolyte brushes with ionizable monomer fractions $f$ at pH=3. (b) Simulation data from the main text showing the brush height $\langle h \rangle$ as a function of the reservoir salt concentration $c_{\text{salt}}^{\text{res}}$ at different pH$^{\text{res}}$ for polyelectrolyte brushes with ionizable monomer fractions $f$ at pH=3. Uncertainties are smaller than the symbol size. As discussed in the main text, direct comparison between experiment and simulation is complicated by several factors. Although the polyelectrolyte brushes in the experiments and simulations have similar grafting densities and contain basic monomers with comparable dissociation constants, the molecular weights of the grafted polymer chains are very different. It is only computationally feasible to simulate polyelectrolyte brushes with relatively short chains ($N = 80$ monomers in this case), whereas the chain length in the experimental systems is not known precisely but is estimated to be at least an order of magnitude larger ($N > \mathscr{O}(10^3)$ monomers). Moreover, to account for sample-to-sample variations in molecular weight, the experimental study reports a normalized brush height, the swelling ratio $h_{\text{wet}}/h_{\text{dry}}$ (defined as the ratio of the solvated $h_{\text{wet}}$ brush height to the dry brush thickness $h_{\text{dry}}$). By contrast, the simulations measure the absolute brush height $\langle h \rangle$, determined by integrating over the monomer density profile, and a dry reference state is not well defined in the context of the implicit-solvent simulations. Thus, it is non-trivial to renormalize the data from experiment and simulation onto the same physical scale (i.e., they are plotted using different scales on the y-axes). Lastly, the experimental systems exhibit brush height hysteresis when pH sweeps are performed in increasing or decreasing directions, whereas the simulated systems do not. Thus, the experimental measurements probe the brush's out-of-equilibrium response, whereas the simulations probe reversible equilibrium behavior. For the specific comparison above, this last issue has been mitigated by choosing pH conditions that fall outside of the region of hysteresis for the experimental system, where the measurements are approximately reversible and thus thought to reflect equilibrium behavior.